

Article

Combined Genome-Wide Association Studies (GWAS) and Linkage Mapping Identifies Genomic Regions Associated with Seedling Root System Architecture (RSA) under Different Nitrogen Conditions in Wheat (*Triticum aestivum* L.)

Yulin Jia, Ninglu Xu, Jun Zhang, Kaiming Ren, Jinzhi Wu, Chunping Wang, Ming Huang and Youjun Li *

College of Agriculture, Henan University of Science and Technology, Luoyang 471023, China; 220410170039@stu.haust.edu.cn (Y.J.); huangming@haust.edu.cn (M.H.)

* Correspondence: lyj@haust.edu.cn

Abstract: The nitrogen (N) use efficiency (NUE) in the roots of seedlings is beneficial for increasing crop yield. Creating marker-assisted selection for wheat root traits can assist wheat breeders in choosing robust roots to maximize nutrient uptake. Exploring and identifying the effect of different N supply conditions on root system architecture (RSA) is of great significance for breeding N efficient wheat varieties. In this study, a total of 243 wheat varieties native to the Yellow and Huai Valley regions of China were utilized for genome-wide association studies (GWAS). Furthermore, a recombinant inbred line (RIL) population of 123 lines derived from the cross between Avocet and Chilero was utilized for linkage examination. A hydroponic seedling experiment using a 96-well tray was conducted in the lab with two treatments: normal N (NN) and low N (LN). Five RSA traits, including the relative number of root tips (RNRT), relative total root length (RTRL), relative total root surface area (RTRS), relative total root volume (RTRV), and relative average root diameter (RARD), were investigated. GWAS and linkage analysis were performed by integrating data from the wheat 660 k single nucleotide polymorphism (SNP) chip and diversity arrays technology (DArT) to identify genetic loci associated with RSA. The results showed that, based on the ratio of RSA-related traits under two N supply conditions, a total of 497 SNP markers, which are significantly associated with RSA-related traits, were detected at 148 genetic loci by GWAS. A total of 10 QTL loci related to RSA were discovered and identified by linkage mapping. Combining two gene localization methods, three colocalized intervals were found: *AX-95160997/QRtrl.haust-3D*, *AX-109592379/QRnrt.haust-5A*, and *AX-110924288/QRtrl.haust-7D/QRtrs.haust-7D*. According to the physical location of the colocalization of these two sites, between 39.61 and 43.74 Mb, 649.97 and 661.55 Mb, and 592.44 and 605.36 Mb are called *qRtrl-3D*, *qRnrt-5A*, and *qRtrl-7D*. This study has the potential to enhance the effectiveness of selecting root traits in wheat breeding programs, offering valuable insights into the genetic underpinnings of NUE in wheat. These results could help in breeding wheat varieties with higher NUE by implementing focused breeding strategies.



Citation: Jia, Y.; Xu, N.; Zhang, J.; Ren, K.; Wu, J.; Wang, C.; Huang, M.; Li, Y. Combined Genome-Wide Association Studies (GWAS) and Linkage Mapping Identifies Genomic Regions Associated with Seedling Root System Architecture (RSA) under Different Nitrogen Conditions in Wheat (*Triticum aestivum* L.). *Agriculture* **2024**, *14*, 1652. <https://doi.org/10.3390/agriculture14091652>

Academic Editor: Rodomiro Ortiz

Received: 17 July 2024

Revised: 3 September 2024

Accepted: 18 September 2024

Published: 21 September 2024

Keywords: *Triticum aestivum* L.; root system architecture; N use efficiency; GWAS; linkage mapping; 660K SNP chip; DArT



Copyright: © 2024 by the authors. Licensee MDPI, Basel, Switzerland. This article is an open access article distributed under the terms and conditions of the Creative Commons Attribution (CC BY) license (<https://creativecommons.org/licenses/by/4.0/>).

1. Introduction

Wheat stands as the most extensively cultivated grain globally, comprising 20% of the world's human dietary intake of calories and protein. By 2050, the world's population is projected to exceed 9 billion, leading to a 60% increase in wheat demand as compared to 2020 [1]. Nitrogen (N) is a key component of various basic functions of plants, such as chlorophyll synthesis, protein formation, nucleic acid production, enzyme activity, alkaloid synthesis, hormone regulation, and vitamin synthesis, all of which play important roles. N is usually the main yield-limiting factor in crop production [2,3]. Proper use of N fertilizer

can greatly enhance crop yield, while overapplication of N fertilizer not only raises production costs but also leads to significant environmental pollution issues. Improving the N use efficiency (NUE) of wheat can achieve high yields and promote environmental protection and sustainable development. Integrating the significance of breeding wheat varieties with high NUE is important in China. Various research studies have demonstrated that the efficiency of crop NUE largely depends on root system architecture (RSA), and the presence and spread of external N sources can, in return, modify the RSA of crops [2]. Therefore, the wheat RSA response to external N levels may represent a pivotal avenue to enhance NUE. Historically, breeders have primarily assessed NUE based on aboveground phenotypic traits, overlooking the critical role of underground roots. This limited perspective has hindered the advancements in high-yield wheat breeding to some extent [3–6].

Many studies have shown that the RSA is crucial in the growth and development of wheat [3,7,8]. RSA encompasses the structural and spatial characteristics of the root system, encompassing traits such as total root length (TRL), total root surface area (TRS), total root volume (TRV), number of root tips (NRT), and average root diameter (ARD) [3,5]. RSA is intricately linked to physiological aspects like N absorption and transport [4,6,9], and exhibits a significant positive correlation with plant N uptake and utilization capacity [6,10]. Thus, RSA has been used as an important index for associating N efficient varieties in rice [11], wheat [12,13], and maize [14,15].

Linkage analysis, sometimes referred to as QTL mapping, is a common technique for examining how quantitative traits are inherited. Compared with traditional linkage analysis, GWAS takes natural population as materials, with a wide range of sources (wild species, local varieties, modern varieties, and high generation strains), high gene polymorphisms, and no need to build a parental population. RSA is a common complex quantitative trait influenced by multiple genes. Combined GWAS and linkage mapping are powerful tools for detecting genes and linkage analysis under complex traits [16]. Because of the restricted genetic diversity in the parental populations, numerous QTLs are unable to be identified [17–19]. Compared with linkage analysis, GWAS are more efficient and provide higher resolution in identifying gene loci. Moreover, combining linkage analysis with GWAS can improve the credibility of the results. This approach has been used to study agronomic characteristics, abiotic stress factors, and genes related to disease resistance in maize [20], cucumber [21], and Brassica napus [22]. In two recent studies, GWAS and linkage analysis were simultaneously used to identify genomic regions of drought resistance [23,24]. Herein, we conducted a lab hydroponic seedling experiment using a GWAS panel (243) and RIL population (123) to investigate the RSA traits associated with various genotypes during the seedling stage under the conditions of normal N (NN) and low N (LN) supply. Then, a comprehensive analysis of the GWAS panel for GWAS, and the RIL population was utilized for linkage examination and confirmation of the hereditary loci distinguished by GWAS, and the important genomic regions related to N response in wheat were identified through GWAS and linkage analysis. This study analyzed different characteristics of RSA to pinpoint genes associated with NUE, offering insight for developing high NUE wheat cultivars.

2. Materials and Methods

2.1. Plant Materials

This study used two wheat panels. Panel I: A total of 243 wheat varieties native to the Yellow and Huai Valley regions of China were utilized for GWAS (Table S1) [25]. Panel II: The F₆ RIL population of 123 lines derived from the cross between Avocet and Chilero parentals are the wheat backbone parent from the International Maize and Wheat Improvement Center (CIMMYT, Mexico, Mexico) [26,27]. This CIMMYT RIL population was previously utilized to study resistance to leaf rust and stripe rust [27].

2.2. Experimental Design and Trail Management

The nutrient solution culture method was used in a seedling stage test. The nutrient solution was referred to Hoagland et al.'s [28] nutrient solution and appropriately modified according to the nutritional characteristics of wheat (Table 1). Two treatments of normal N (NN, 4.0 mmol/L) and low N (LN, 0.8 mmol/L) were set in the laboratory. The LN nutrient solution contained the same nutrients concentration as the NN nutrient solution except for the concentration of $\text{Ca}(\text{NO}_3)_2$ with 0.4 mmol/L, CaCl_2 with 2.1 mmol/L, and $(\text{NH}_4)_2\text{SO}_4$ with 0 mmol/L. The pH of nutrition solution was adjusted to 6.0 with dilute HCl and NaOH before transferring. Wheat grains were soaked in a 10% H_2O_2 solution for 10 min, and seeds were germinated in saturated CaSO_4 solution for 7 days at 20 °C. Once the seedlings reached the one-leaf stage and exhibited similar growth, the germinated seeds with residual endosperm removed were transferred to black 96-well seedling tray (12.7 cm long \times 11.4 cm wide \times 8.7 cm high, diameter of 6.3 mm and 12 holes per row), containing 800 mL of nutrient solution. The seedlings were randomly placed with five replications of each variety and grown in a intelligent artificial climate chamber (Zhejiang Top Clou-agri Technology Co., Ltd., Hangzhou, China). The climate setting was 14 h in light with a light intensity of 3000 Lx and a temperature of 25 °C and 10 h in darkness with a light intensity of 0 Lx and a dark temperature of 18 °C, with a humidity of 60%. The solution was changed every 3 days. All experiments were completed in three batches.

Table 1. Components of nutrient solution for wheat seedling culture.

Macronutrients	Trait		Trace Elements	Trait	
	NN (mmol/L)	LN (mmol/L)		NN (mmol/L)	LN (mmol/L)
KCl	1.8	1.8	H_3BO_3	1×10^{-3}	1×10^{-3}
CaCl_2	1.5	2.1	ZnSO_4	1×10^{-3}	1×10^{-3}
$\text{Ca}(\text{NO}_3)_2$	1	0.4	MnSO_4	1×10^{-3}	1×10^{-3}
$(\text{NH}_4)_2\text{SO}_4$	1	0	CuSO_4	0.5×10^{-3}	0.5×10^{-3}
MgSO_4	0.5	0.5	Fe-EDTA	0.1	0.1
KH_2PO_4	0.2	0.2	$(\text{NH}_4)_6\text{Mo}_7\text{O}_{24}$	1.0×10^{-4}	1.0×10^{-4}

2.3. Trait Measurements

Following 21 days of cultivation, the roots were washed with deionized water before being trimmed at the segmented points using scissors, and were placed in a transparent tray for testing. Five individual plants were randomly selected from each sample, and the lateral roots of each plant were separated one by one, placed in a transparent root tray containing deionized water in a non-overlapping state, and the root system was scanned by the WinRHIZOLA6400XL (Regent Instruments Inc., Quebec Canada) perspective scanning system to obtain the root system pictures of each individual plant. Then the WinRHIZOPro 5.0 software was used to analyze the RSA traits of each sample, such as total root length (TRL), total root surface area (TRS), total root volume (TRV), number of root tips (NRT), and average root diameter (ARD), and these phenotypic data of each material were determined by calculating the average of five replicates. Subsequently, the relative values of each trait under the two different N supply conditions were calculated, namely, RNRT, RTRL, RTRS, RTRV, and RARD. Origin 2021 (Originlab, Northampton, USA) was used to statistically analyze the data, and the correlation coefficient was calculated using SPSS 22.0 (IBM Inc., Chicago, USA) and Kolmogorov–Smirnov (K–S test) for normality testing. If $p > 0.05$, it indicates that the sample data are normally distributed, and can be used for a paired sample *t*-test. The heritability of phenotype data were calculated using the Lem4 package (<https://github.com/lme4>, accessed on 24 May 2024) according to Zhao et al. [29]. The calculated genetic variance V_g , environmental variance V_e , and genotype year interaction variance V_{ge} are introduced into the heritability calculation formula for heritability calculation.

$$H = V_g / (V_g + V_{ge}/e + V_e/re)$$

where r is the number of replicates in one environment and e is the number of environments.

2.4. GWAS

The 660 k gene chip data of the GWAS panel were analyzed by Beijing CapitaBio Technology Co., Ltd., Beijing, China (<http://capital.en.drugdu.com>, accessed on 20 January 2024) [25]. The quality pretreatment of genotyping data was carried out for SNP call rate and MAF (minor allele frequency) with the PLINK 1.9 software with threshold of maf 0.02 and geno 0.1 (<http://zzz.bwh.harvard.edu/plink/tutorial.shtml>, accessed on 10 February 2024), resulting in the retention of 395,782 SNPs. Tassel v5.0 (<https://www.maizegenetics.net/tassel>, accessed on 10 February 2024) was used for PCA and kinship analysis. The mixed linear model (MLM) in Tassel V5.0 software was used for GWAS. The model principle is as follows [25,30,31].

$$Y = X\alpha + Q\beta + K\mu + \varepsilon,$$

Phenomenal attributes are denoted by Y , genotype by X , and principal components matrix (Q) by the first three principal components. The kinship matrix is K ; corresponding effects are α , β , and μ ; residual effects are represented by the matrix ε . The matrices X and Q are regarded as fixed effects, while the matrices K and ε are regarded as random effects.

To combine the GWAS results from all traits, a uniform suggestive genome-wide significance threshold $-\log_{10}(p\text{-value}) > 5$ was used according to previous studies [22,23,29,32]. To reduce false positives, the online software BioLadder (<https://www.bioladder.cn/web/#/chart/58>, accessed on 25 August 2024) Perform FDR (false discovery rate) calibration was used. Using the BH (Benjamini and Hochberg) method, FDR correction was applied to the p -value, with the cut-off standard being $FDR < 0.05$ after correction. When suggestive genome-wide significance threshold $-\log_{10}(p\text{-value})$ is >5 and FDR is <0.05 , it is considered a significant SNP site. We also used R package q -value [33] to calculate the q value corresponding to the p value (Table S2).

Linkage disequilibrium (LD) among markers was calculated for the whole genomes in PLINK software [34]. Using the CMplot program in the R 4.22 package, Manhattan and quantile–quantile (Q–Q) plots were made.

2.5. Linkage Analysis

According to Zhao's genetic linkage map data [29], a high-density genetic linkage map was created from the whole genomes of the RIL population and its two parents using a wheat DArT array. The map covers 21 wheat chromosomes and is 8202.10 cM long. It features 3627 DArT markers spaced 2.26 cM apart on average. The QTLs of the RSA trait were mapped using the composite interval mapping approach with the LOD threshold set to 2.5 using the BIP function of the QTL IciMapping V4.2 program [23,29,35,36]. According to the results obtained from IciMapping V4.2, MapChart V2.32 software was used to map the Quantitative Trait Locus (QTL) linkage group [37]. The QTL names were assigned using McCouch's methodology [38].

3. Results

3.1. Phenotypic Evaluation

The results (Table 2) showed that in the two populations, different RSA indexes of wheat showed certain variability, and the range of the coefficient of variation (CV) was different. Under the NN condition, the CV of each character in the GWAS panel ranged from 11.39% (ARD) to 39.72% (TRL), and in the RIL population, they ranged from 14.29% (ARD) to 48.98% (TRS). Under the LN condition, the CV of each character of the GWAS panel ranged from 26.36% (ARD) to 54.19% (NRT) and of the RIL population ranged from 16.39% (ARD) to 55.09% (TRS). The relative ratios of all RSA traits were greater than 1 except RARD (0.98) in the GWAS panel. The CV of relative ratios in the GWAS panel ranged from 29.24% (RARD) to 52.26% (NRT) and in the RIL population ranged from 14.78% (RARD) to 46.62% (RNRT).

Table 2. Summary of RSA traits in different populations under different nitrogen levels.

Treatment	Trait	GWAS Panel					RIL Population				
		Min.	Max.	Average	Standard Deviation	CV (%)	Min.	Max.	Average	Standard Deviation	CV (%)
NN nutrient solution	TRL (cm)	60.07	372.1	143.72 **	57.09	39.72	58.19	279.43	132.28 *	53.46	40.41
	TRS (cm ²)	14.13	135.1	51.73 **	19.59	37.87	19.29	209.41	45.27	22.16	48.95
	ARD (mm)	0.67	1.62	1.15 *	0.13	11.39	0.84	2.3	1.08 **	0.15	14.29
	TRV (cm ³)	0.25	3.9	1.5 **	0.58	38.95	0.45	2.52	1.18	1.08	37.14
	NRT	38	293	91 **	35.6	39.2	23	214	81	33.16	41.15
LN nutrient solution	TRL (cm)	80.12	474.4	237.38	89.54	37.72	66.91	290.3	146.09	55.6	44.09
	TRS (cm ²)	20.3	159.3	77.71	27.42	35.29	18	232.67	44.35	24.43	55.09
	ARD (mm)	0.23	2.31	1.11	0.29	26.36	0.84	2.55	1.13	0.19	16.39
	TRV (cm ³)	0.09	4.54	1.91	0.85	44.62	0.38	2.48	1.17	1.32	40
	NRT	43	457	134	72	54.19	29	171	82	33	39.88
Relative ratio	RTRL	0.93	5.68	1.8	0.83	45.88	0.31	2.45	1.05	0.46	44.34
	RTRS	0.79	5.68	1.62	0.69	42.8	0.34	2.42	1.06	0.46	42.95
	RARD	0.2	2.22	0.98	0.29	29.24	0.69	1.64	1.06	0.16	14.78
	RTRV	0.06	5.61	1.4	0.78	55.72	0.36	2.66	1.1	0.5	45.57
	RNRT	0.73	5.58	1.56	0.82	52.26	0.27	3.02	1.13	0.53	46.62

Note: ** indicates significantly different level of NN and LN paired *t*-test at $p < 0.01$ level. * indicates significantly different level of NN and LN paired *t*-test at $p < 0.05$ level. We converted non-normally distributed samples into natural logarithmic values ($\ln(x)$) for comparison (total root length (TRL), total root surface area (TRS), total root volume (TRV), number of root tips (NRT), average root diameter (ARD), relative number of root tips (RNRT), relative total root length (RTRL), relative total root surface area (RTRS), relative total root volume (RTRV), relative average root diameter (RARD)).

Genetic analysis revealed the genotype, environmental, and genotype \times environment interaction variance of the five RSA traits, indicating that each trait is not only influenced by genotype, but also by environment (Table S3). In the GWAS panel, the heritability of the five RSA traits ranges from 0.689 to 0.429, with TRL and TRS having higher heritability of 0.689 and 0.688, respectively. In the RIL population, the heritability ranges from 0.867 to 0.483, with ARD, TRS, and TRV having the higher heritability of 0.867, 0.733, and 0.710, respectively. These results indicate that the environment has a relatively small impact on these traits and is mainly controlled by genetic factors. Comparing the two populations, it can be found that except for TRL, the heritability of the other four traits in the RIL population is greater than that in the GWAS panel, indicating that the RIL population is more strongly influenced by genetic factors, while the GWAS panel is more strongly influenced by environmental factors.

The normality test results indicated that for the TRL and TRS in RIL populations, the RSA traits followed a normal distribution ($p > 0.05$) except for the TRL under NN, TRS under LN, and NRT in the GWAS panel. However, when applying a natural logarithm transformation, all the traits followed a normal distribution ($p > 0.05$). Thus, we proceeded to conduct a paired *t*-test using the natural logarithm values of these values. The paired *t*-test results showed that LN supply could increase TRL, TRS, and NRT in the GWAS panel, and TRL in the RIL population, and the increase was greater in the GWAS panel than in the RIL population (Table 2 and Figure 1).

Figure 2 shows that the percentages of TRL, TRS, TRV, and NRT were significantly positively correlated in both populations and both N supply conditions ($p < 0.05$), with the correlation coefficient r ranging from 0.19 to 0.95. However, in the GWAS panel, the ARD was negatively correlated with TRL and NRT in the two N supply conditions ($p < 0.05$), and the correlation coefficient r ranged from -0.46 to -0.18 , while in the RIL population, it was only negatively correlated in the NN treatment ($p < 0.05$).

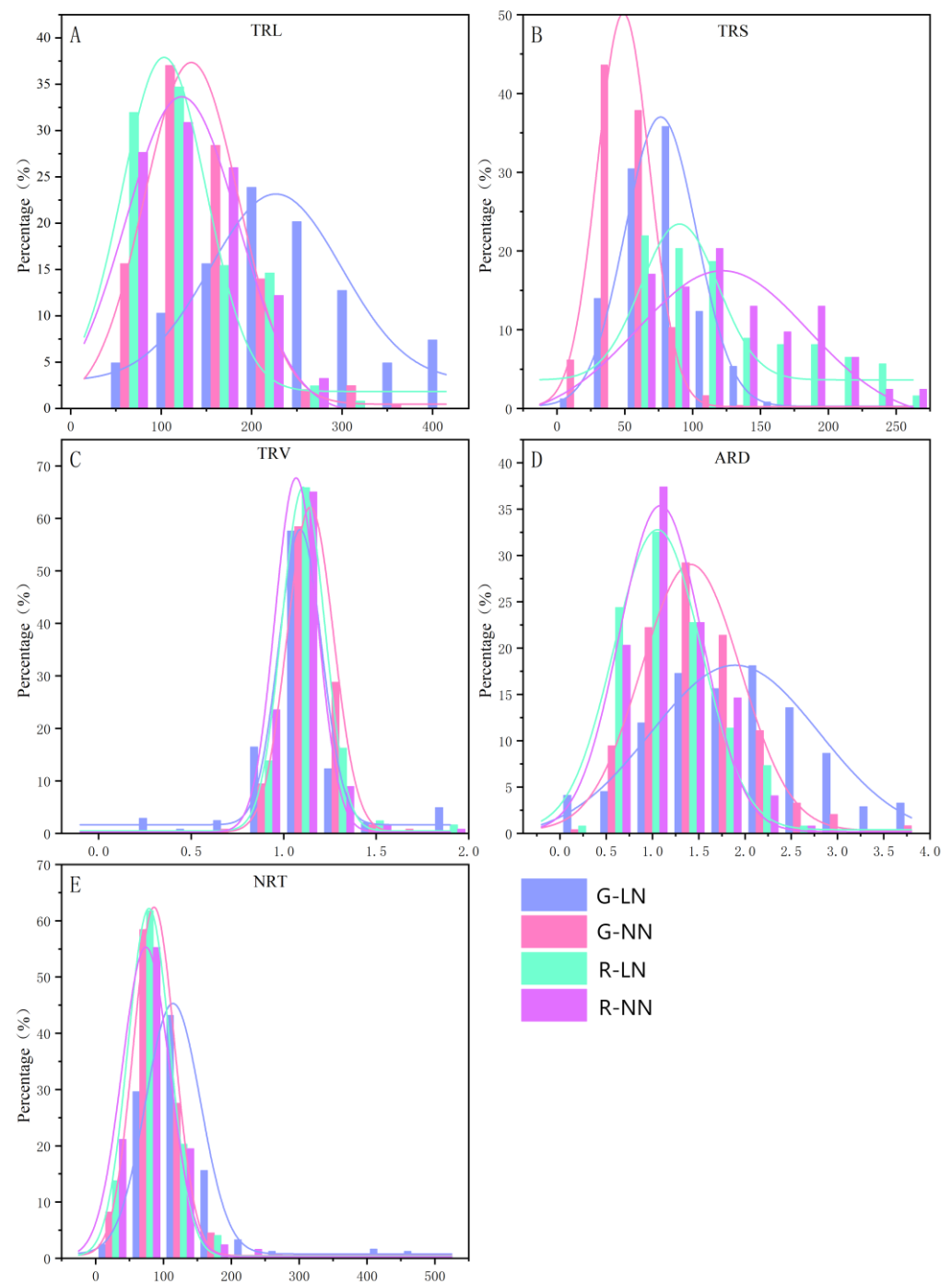


Figure 1. Phenotype distribution map of the GWAS panel and the RIL population. G-LN: The GWAS panel under low N treatment; G-NN: The GWAS panel under normal N treatment; R-LN: The RIL population under low N treatment; R-NN: The RIL population under normal N treatment. Total root length (TRL (A)), total root surface area (TRS (B)), average root diameter (ARD (C)), total root volume (TRV (D)), and number of root tips (NRT (E)).

Figure 3 shows that the RSA performances of Avocet and Chilero were quite different under NN and LN conditions. The *t*-test results of the RIL population parents showed that under the NN condition, the TRL, TRS, TRV, and NRT of Avocet were all greater than Chilero ($p < 0.05$), while there was an opposite tendency under the LN condition. These results reflect that the RSA responses to parents (Avocet and Chilero) were significantly different under different N supply.

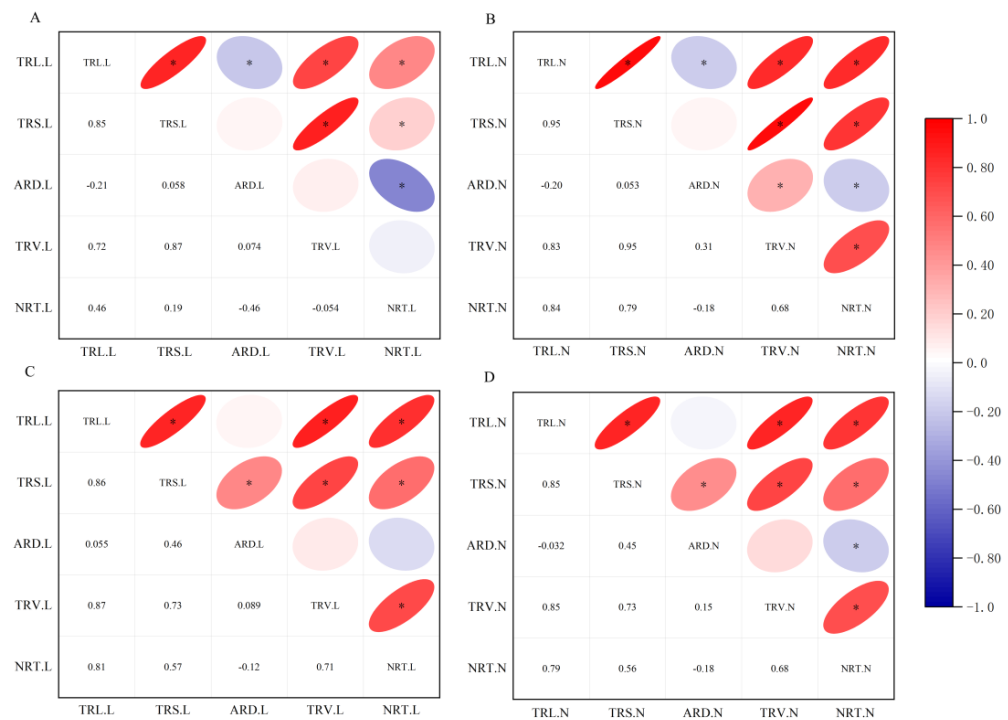


Figure 2. Pearson correlation map between variables of the GWAS panel under LN treatment (A), GWAS panel under NN treatment (B), RIL population under LN treatment (C), and RIL population under NN treatment (D). TRL.L: total root length under LN treatment; TRL.N: total root length under NN treatment; TRS.L: total root surface area under LN treatment; TRS.N: total root surface area under NN treatment; TRV.L: total root volume under LN treatment; TRV.N: total root volume under NN treatment; ARD.L: average root diameter under LN treatment; ARD.N: average root diameter under NN treatment; NRT.L: number of root tips under LN treatment; NRT.N: number of root tips under NN treatment. * refers to the different significance at $p < 0.05$ level, respectively.

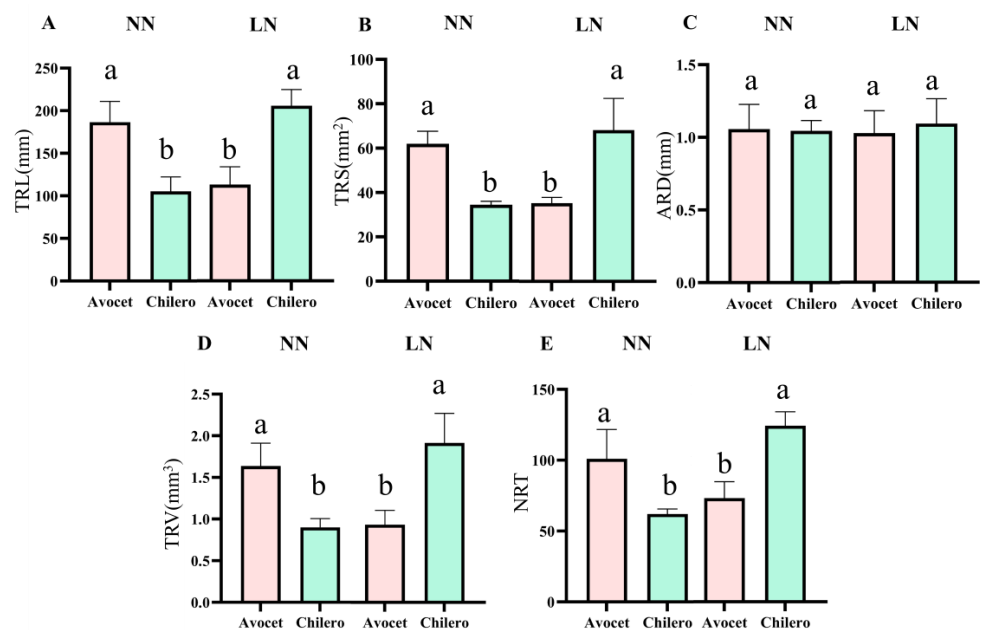


Figure 3. Effects of different treatments on the average total root length (TRL (A)), total root surface area (TRS (B)), average root diameter (ARD (C)), total root volume (TRV (D)) and number of root tips (NRT (E)) of Avocet and Chilero. Different lowercase letters on the bar indicate significant differences between different of Avocet and Chilero ($p < 0.05$). Normal N (NN) and low N (LN).

3.2. GWAS Analysis

The quantile–quantile (Q–Q) plots indicated that the false positives were well controlled in GWAS models (Figure 4). There were 497 SNP markers that were substantially linked to features relevant to N use efficiency. Based on the attenuation distance of whole genome linkage disequilibrium (LD), the 10 Mb intervals before and after significant SNPs were identified as QTL sites (Figure S1). These SNPs were distributed across 148 genetic loci (Figure 4 and Table S2). Ten loci were linked to RTRL, accounting for 8.0~15.6% of the phenotypic variation; seventy loci were linked to RTRS, accounting for 9.1~26.9% of the variation; sixty-seven loci were linked to RTRV, accounting for 9.1~19.8% of the variation; sixty-three loci were linked to RARD, accounting for 8.2~24.7% of the variation; and seventy-nine loci were linked to RNRT, accounting for 8.9~15.2% of the phenotypic variation. There was a high correlation between the ratio of two RSA traits under the two N supply conditions. Among these loci associated with RSA, four loci were associated with RTRS and RNRT, one locus was associated with RTRS, RTRV, thirty-one loci were associated with RTRS, RTRV, and RNRT, one locus was associated with RTRS and RNRT, six loci were associated with RTRL, RTRS, RTRV, and RNRT, twelve loci were associated with RTRS, RTRV, and RNRT, and three loci were associated with RTRL, RTRS, RTRV, and RNRT.

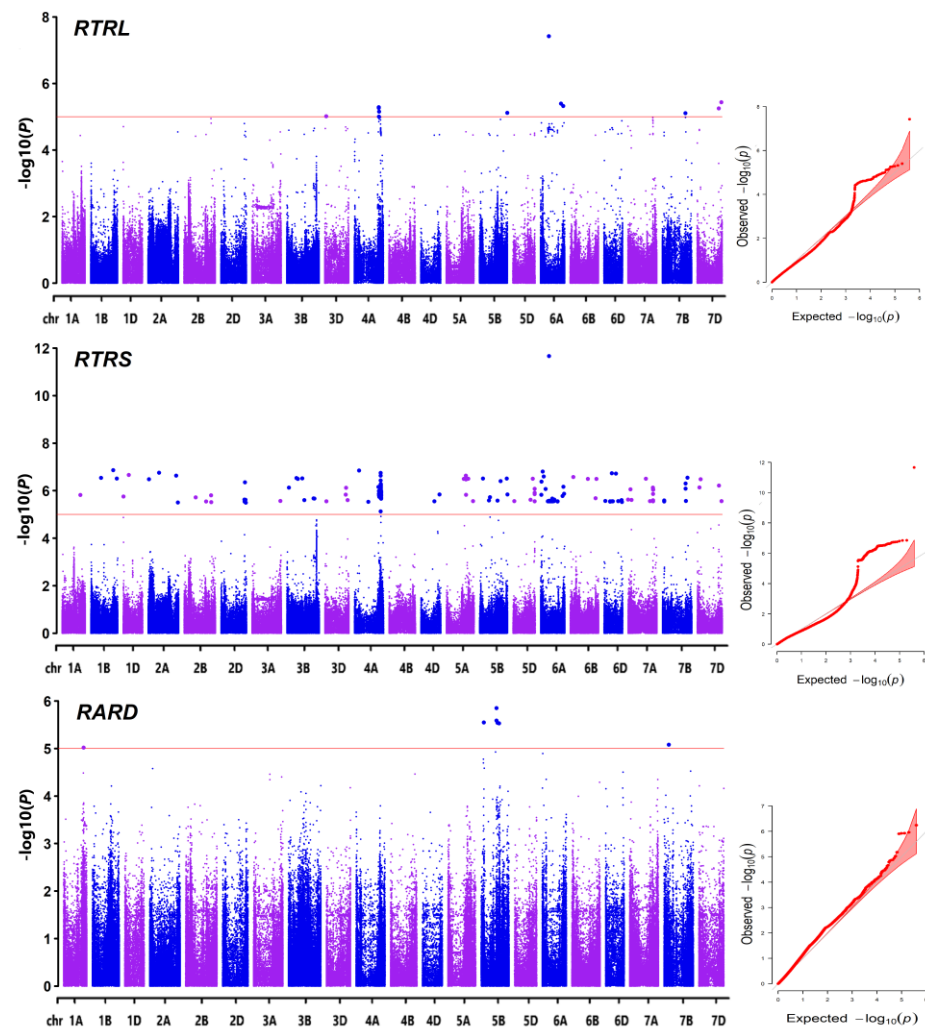


Figure 4. Cont.

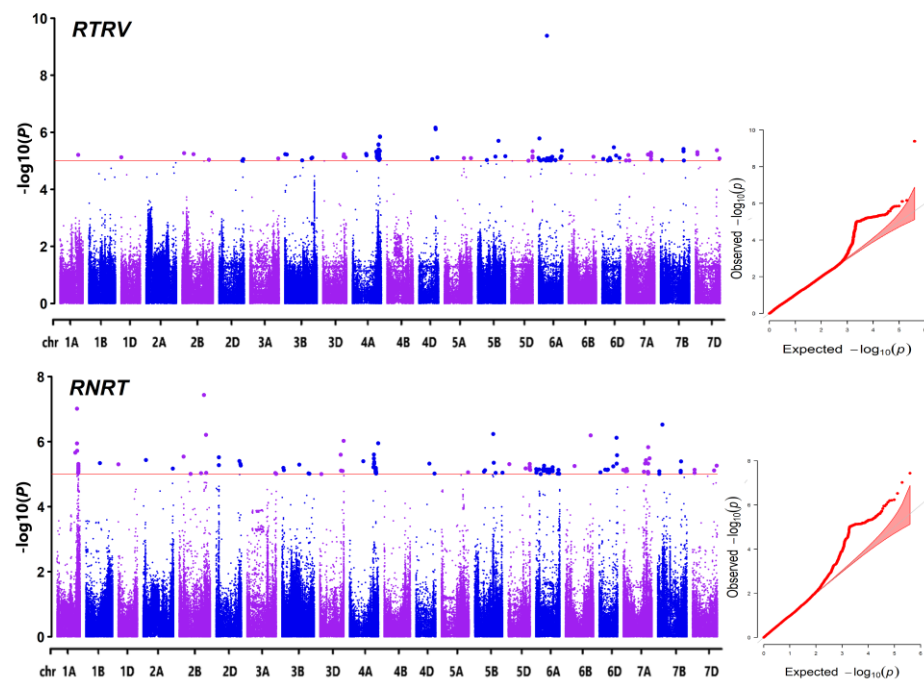


Figure 4. GWAS of relative ratios of RSA of GWAS panel under different N conditions using Manhattan plot and Q–Q plot. The points in the figure represent SNP markers. Relative number of root tips (RNRT), relative total root length (RTRL), relative total root surface area (RTRS), relative total root volume (RTRV), and relative average root diameter (RARD).

3.3. Linkage Mapping

As shown in Figure 5 and Table 3, three QTLs were found to be linked to RTRL, with the LOD values ranging from 3.15 to 5.16, explaining 7.58% to 15.04% of the phenotypic variances. Two QTLs were found to be linked to RTRS, with the LOD values ranging from 3.71 to 4.16, explaining 10.22% to 15.92% of the phenotypic variances. Two QTLs were found to be linked to RARD, with the LOD values ranging from 2.52 to 3.95, explaining 8.16% to 13.72% of the phenotypic variances. One QTL was found to be linked to RNRT, with an LOD value of 2.89, explaining 10.3% of the phenotypic variances.

Table 3. Linkage analysis results.

Trait Name	QTL	Position (MB)	Left Marker	Right Marker	LOD	PVE (%)	Add
RTRL	QRtrl.haust-3A	3418	DarT3934005	DarT4005016	5.16	15.05	−0.2315
RTRL	QRtrl.haust-3D	57	DarT2260219	DarT1145273	3.15	7.58	−0.142
RTRL	QRtrl.haust-7D	1322	DarT2245918	DarT100437414	4.76	11.23	0.1876
RTRS	QRtrs.haust-3A	3416	DarT3934005	DarT4005016	4.16	15.92	−0.2275
RTRS	QRtrs.haust-7D	1322	DarT2245918	DarT100437414	3.71	10.22	0.1725
RARD	QRard.haust-4B	1292	SNP1215980	SNP100022040	3.95	13.72	−0.0572
RARD	QRard.haust-6B	417	SNP100562446	SNP100562447	2.52	8.16	−0.0441
RTRV	QRtrv.haust-2B	1149	SNP2263629	SNP100542876	2.96	9.71	0.156
RTRV	QRtrv.haust-7D	1323	DarT100437414	DarT3034325	2.93	9.93	0.1743
RNRT	QRtrl.haust-5A	249	SNP100260537	SNP1722105	2.89	10.27	−0.176

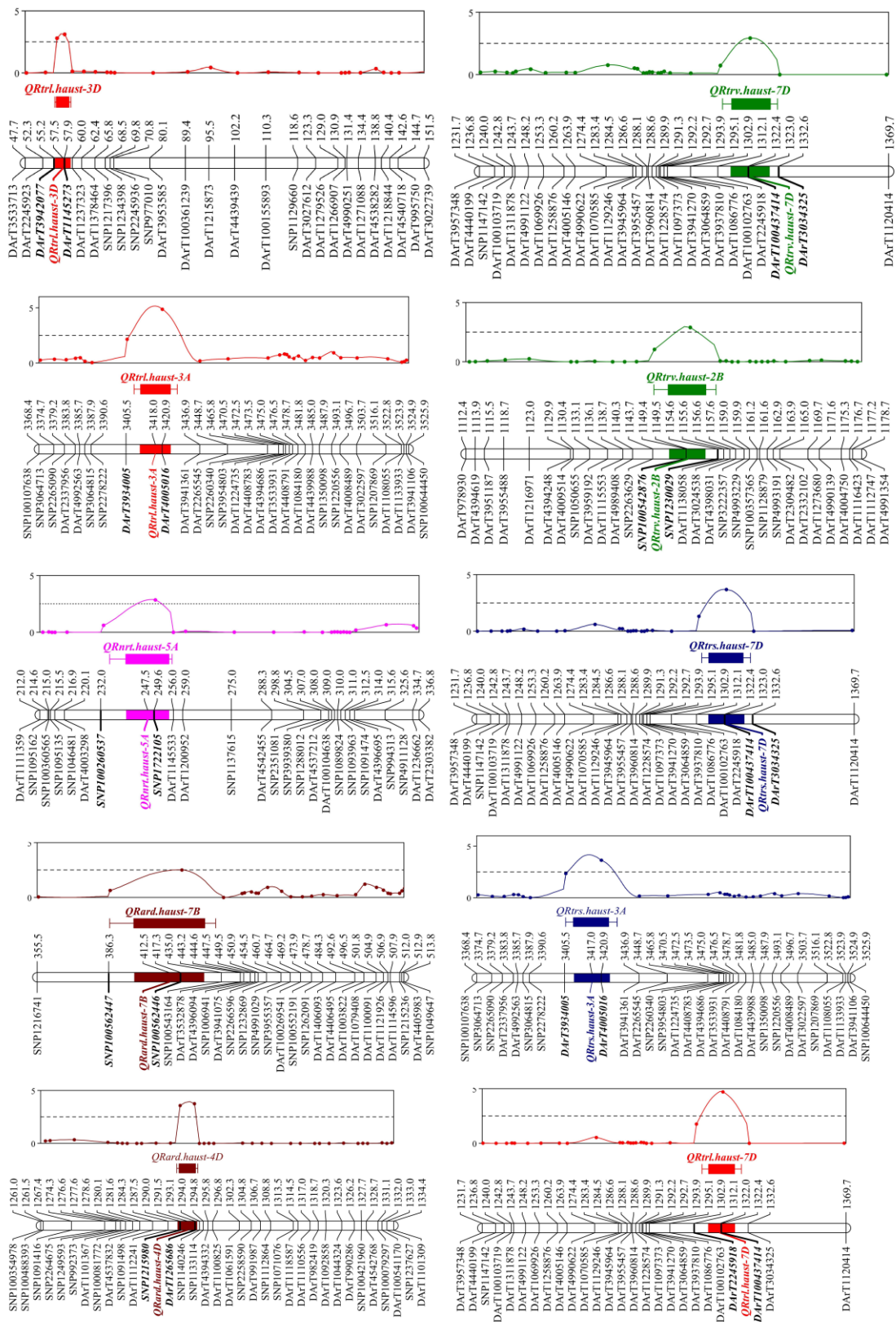


Figure 5. Distribution of QTLs related to RSA on chromosomes. The names of marker loci and QTLs are listed next to the corresponding chromosomes, indicated in bold italic font. To the right of the chromosome map is the LOD distribution map, including all markers with LOD peaks greater than 2.5.

3.4. Colocalized Gene Regions

Using GWAS and linkage mapping, three important RSA-related QTLs were found (Table 4). The significant marker AX-95160997 obtained through GWAS analysis of RTRL loci is located within the significant QTL QRtrl.haust-3D obtained through linkage analysis, with a physical interval of 39.61–43.74 Mb. The significant marker AX-109592379 associated with RNRT is located within the significance QTL QRnrt.haust-5A, with a physical interval of 649.97–661.55 Mb. The significant marker AX-110924288 associated with RTRL and RTRS is located in QRtrl.aust-7D and QRtrs.haust-7D, with a physical interval of 592.44–605.36 Mb.

Table 4. Colocalized gene regions.

Trait Name	Chr	Loci	Physical Interval (Mb)	PVE (%)
RTRL	3D	AX-95160997/QRtrl.haust-3D	39.61–43.74	7.58–9.14
RNRT	5A	AX-109592379/QRnrt.haust-5A	649.97–661.55	10.27–10.81
RTRL, RTRS	7D	AX-110924288/QRtrl.haust-7D/QRtrs.haust-7D	592.44–605.36	9.95–11.22

4. Discussion

4.1. Effect of RSA on NUE

Wheat yield is significantly impacted by RSA. Studies have shown that traits such as root length, diameter, and absorption area of the root system are significantly positively correlated with yield traits such as thousand grain weight, grain length, and grain width [2,3,7,8]. Breeders partially complete the selection of wheat RSA by indirect methods such as the artificial breeding process to aggregate high-yield genes and choose high-yield materials [39]. In this trial, we found that the RSAs were different between the two populations and among the varieties in the same populations, and there was a high correlation among the ratios of each two RSA traits under both the two N supply conditions. These results provide a basis for indirectly exploring NUE-related loci by carrying out the identification of RSA under different N supply conditions and promoting the selection and breeding of wheat with high NUE.

The developed root system is the basis of efficient N absorption and utilization. The more developed the root, the thinner the average diameter of the root [40]. The more fine roots that are related to the root tips, the longer the TRL, the larger the TRS, and the more conducive for capture of N from soil by plants [41,42]. Crops with different N efficiency not only have different performance in N accumulation, but also have different root morphological and quantitative properties [2,43]. Previous researchers have demonstrated that higher TRS means N efficiency in wheat [2,44]. Other studies also found that N efficient rice had substantially higher TRL, TRS, and TRV than N inefficient rice [45,46]. In this research, LN supply could increase TRL, TRS, and NRT in the GWAS panel, and TRL in in RIL population, which was consistent with the previous research results [2,43]. Moreover, the CV of the GWAS panel is greater than that of the RIL population, which may be related to the richer genetic diversity of the GWAS panel. These results prove that the elongation of most materials' roots can be promoted under low N stress. Moreover, our study found that ARD was negatively correlated with TRL, TRS, TRV, and NRT, suggesting that the smaller ARD of roots is better for developing wheat roots.

The response of wheat root RSA to low N stress has been widely utilized to dig wheat NUE genes [2,32]. It can correctly locate the RSA genes affected by low N and better depict the reaction of plant seedling roots to low N environment [2,35,47]. All CVs of the RSA traits except ARD were greater than 20%, indicating that RSA traits are closely related to the genotype of the material. The CVs of the relative proportion of RSA in the GWAS panel and the RIL population were more than 40% except for RARD, indicating that under low N stress, there are great differences in the RSA of wheat genotypes, and different genotypes have different responses to low N supply. This result is in accordance with previous research outcomes [2].

4.2. Linkage Analysis and GWAS Together Offer a Novel Method for Identifying the Genes Causing RSA

Previous studies mapped QTL loci for traits related to NUE under field conditions; however, relatively limited genetic variation in the parental population resulted in a large physical distance [48,49]. To reduce QTL intervals by raising marker density inside candidate segments, QTL mapping is typically necessary [50,51]. The process of genetically analyzing quantitative traits has been greatly aided in recent years by the invention and application of wheat gene chips [52]. Numerous QTLs and QTL clusters have also been found in various wheat N treatment trials [2,36,43,47,53–56]. In this study, the wheat 660 k SNP chip and DArT technology were used to analyze the inheritance of RSA during the wheat seedling stage, employing GWAS and QTL mapping under different N levels. The loci significantly associated with RSA were distributed on the 21 chromosomes. Some of these loci overlapped or coincided with multiple RSA-related loci discovered by Jin et al. [2], Xiong et al. [43], Fan et al. [47], Yang et al. [36], and Ren et al. [56] (Table S4), in which the mapped area contains numerous known NUE-related genes such as NRT2s genes on chromosome 6A, which can be associated with RTRL, RTRS, RNRT, and other traits. In addition, in our genetic mapping interval, we found that several genes related to RSA may be associated with NUE in wheat, including genes NPF6.2, FD-GOGAT, and NR1.2. Within the overlapping intervals identified by both GWAS and QTL mapping, we found the GS2 genes [57–59]. In the genetic mapping interval, we also found an auxin responsive gene. Despite the discovery of genes within the genetic mapping interval, the large size of the candidate gene interval currently prevents us from definitively identifying these genes as the specific candidates of interest. Further refinement of the interval through additional genetic and molecular analyses will be necessary to narrow down the list of potential genes and pinpoint those related to NUE.

Combining GWAS and linkage mapping, we detected a significant locus AX-95160997/*QRtrl.haust-3D* (Table 4), which may be an important NUE locus. According to its colocalized physical location, it is between 39.61 and 43.74 Mb, named as *qRtrl-3D*. In this interval, the Chinese Spring 2.0 database was used to screen high-confidence genes. There are a total of sixty-one annotated genes. Through screening, we found a possible candidate gene *TraesCS3D02G090300*, which is located at 0.05 Mb, flanking the significance marker *DarT1145273* (*QRtrl.haust-3D*). By querying the gene annotation, we found that it encodes an MADS box transcription factor. Previous studies have shown that the MADS box transcription factor plays an irreplaceable role in the process of plant growth and development and signaling. Studies of Arabidopsis showed that the MADS box transcription factor is mainly expressed in roots and regulates lateral root growth and development [60,61] by regulating auxin synthesis [62]. Recent studies have shown that the MADS box transcription factor family play an important role in nitrate supply in roots and is involved in regulating NUE in wheat, which provides a new clue for further exploring the function of this gene on NUE [63,64].

This study also found two colocalized intervals AX-109592379/*QRnrt.haust-5A* and AX-110924288/*QRtrl.haust-7D*/*QRtrs.haust-7D* (Table 4). The physical location of the colocalization of these two sites were 649.97–661.55 Mb and 592.44–605.36 Mb, which were called *qRnrt-5A* and *qRtrl-7D*. Previous studies did not overlap these two intervals, suggesting that they may be two new loci. Candidate genes were screened in the *qRnrt-5A* interval, and some possible candidate genes were listed, such as the *TraesCS5A02G519300* gene, which encodes a protein with the NAC binding domain (Table 5). Studies have shown that overexpression of the NAC transcription factor can significantly increase nitrate influx rate, N uptake, and other traits [65], but it cannot be identified as a candidate gene due to the large candidate interval. Candidate genes were screened in the *qRtrl-7D* interval, and some possible candidate genes were listed, such as the *TraesCS7D02G538000* gene, which encodes an E3 ubiquitin protein ligase. The multitype protein family E3 ubiquitin protein ligase is crucial for root and bud growth and development, as well as plant N absorption [66,67].

Table 5. Candidate gene prediction.

QTL	Gene	Position(Mb)	Gene Annotation or Coding Protein
<i>qRtrl-3D</i>	<i>TraesCS3D02G083600</i>	40.0397–40.4099	F-box protein PP2-B11
	<i>TraesCS3D02G087200</i>	42.06815–42.07455	Rab GTPase-activating protein
	<i>TraesCS3D02G088200</i>	42.92659–42.93343	E3 ubiquitin-protein ligase ATL41
	<i>TraesCS3D02G088300</i>	42.92979–42.93343	Probable LRR receptor-like serine/threonine-protein kinase At3g47570
	<i>TraesCS3D02G088900</i>	42.97653–42.97697	Histone H2B.1
	<i>TraesCS3D02G090300</i>	43.79470–43.79640	MADS-box transcription factor 29
<i>qRnrt-5A</i>	<i>TraesCS5A02G515500</i>	649.19444–649.20657	MADS-box transcription factor 50
	<i>TraesCS5A02G519300</i>	651.00397–651.00821	NAC domain-containing protein 86
<i>qRtrl-7D</i>	<i>TraesCS7D02G521500</i>	592.53732–649.75623	Programmed cell death protein 2
	<i>TraesCS7D02G529200</i>	598.08138–598.08266	Transcription factor bHLH93
	<i>TraesCS7D02G533900</i>	601.2191–601.22013	BTB/POZ and MATH domain-containing protein 2
	<i>TraesCS7D02G538000</i>	603.54478–603.54565	E3 ubiquitin-protein ligase ATL15

With the release of wheat genome sequence, gene function verification and exploration have become an important topic in the post genome era of wheat [2]. However, the widespread phenomenon of one cause and multiple effects in organisms also makes the determination of gene function difficult, which still requires solid gene function verification. At present, bioinformatics analysis based on reliable association markers traits is an effective method to explore candidate genes related to complex agronomic traits. This work detected 10 QTLs, 497 SNP markers, and 3 colocalized gene regions for RSA under different N supply levels. This work provide more candidate gene loci for N efficient molecular breeding, targeted improvement of specific crop subspecies or the creation of excellent new varieties, and providing references for improving NUE.

5. Conclusions

In this study, based on exploring the ratio of RSA traits of GWAS panel and RIL populations under normal N and low N supply conditions, a total of 497 SNP markers associated with RSA traits were detected at 148 genetic loci identified by GWAS, and a total of 10 QTL loci related to RSA traits were discovered identified by linkage mapping. Finally, three significant RSA-related QTL genetic loci, namely, *qRtrl-3D*, *qRnrt-3D*, and *qRtrl-7D*, were mapped according to the responses of RSA traits. In the case of the linkage mapping, the parental contributed positively in the three main NUE QTLs.

Supplementary Materials: The following supporting information can be downloaded at: <https://www.mdpi.com/article/10.3390/agriculture14091652/s1>, Table S1: 243 GWAS panel names; Table S2: Marker-trait associations for N use efficiency related traits ($p \leq 0.0001$); Table S3: Heritability analysis of 5 RSA traits; Figure S1. LD decay analysis of GWAS panel; Table S4: Comparison of the results of previous studies.

Author Contributions: Y.J.: Conceptualization, data curation, formal analysis, writing—original draft, writing—review and editing. N.X.: Data curation, formal analysis, writing—original draft. J.Z.: Investigation, validation, writing—original draft. K.R.: Investigation, validation, writing—original draft. J.W.: Investigation, validation, writing—original draft. C.W.: Project administration, resources, writing—review and editing. Y.L.: Funding acquisition, project administration, resources, supervision, writing—review and editing. M.H.: Project administration, resources, supervision, writing—review and editing. All authors have read and agreed to the published version of the manuscript.

Funding: The authors declare that financial support was received for the research, authorship, and/or publication of this article. This study was financially supported by National Key Research and Development Program of China (under grant no. 2022YFD2300800), the Science and Technology Research Project of Henan, China (under grant no. 232102111009).

Institutional Review Board Statement: Not applicable.

Data Availability Statement: The data that support the findings of this study are available in the main body of the paper.

Conflicts of Interest: The authors declare no conflicts of interest.

References

- Langridge, P.; Alaux, M.; Almeida, N.F.; Ammar, K.; Baum, M.; Bekkaoui, F.; Bentley, A.R.; Beres, B.L.; Berger, B.; Braun, H. Meeting the challenges facing wheat production: The strategic research agenda of the Global Wheat Initiative. *Agronomy* **2022**, *12*, 2767. [[CrossRef](#)]
- Jin, Y.; Liu, J.; Liu, C.; Jia, D.; Liu, P.; Wang, Y. Genome-wide association study of nitrogen use efficiency related traits in common wheat (*Triticum aestivum* L.). *Acta Agron. Sin.* **2021**, *47*, 394–404. [[CrossRef](#)]
- Maccaferri, M.; El-Feki, W.; Nazemi, G.; Salvi, S.; Canè, M.A.; Colalongo, M.C.; Stefanelli, S.; Tuberosa, R. Prioritizing quantitative trait loci for root system architecture in tetraploid wheat. *J. Exp. Bot.* **2016**, *67*, 1161–1178. [[CrossRef](#)] [[PubMed](#)]
- de Dorlodot, S.; Forster, B.; Pagès, L.; Price, A.; Tuberosa, R.; Draye, X. Root system architecture: Opportunities and constraints for genetic improvement of crops. *Trends Plant Sci.* **2007**, *12*, 474–481. [[CrossRef](#)]
- Kabir, M.R.; Liu, G.; Guan, P.; Wang, F.; Khan, A.A.; Ni, Z.; Yao, Y.; Hu, Z.; Xin, M.; Peng, H. Mapping QTLs associated with root traits using two different populations in wheat (*Triticum aestivum* L.). *Euphytica* **2015**, *206*, 175–190. [[CrossRef](#)]
- Bishopp, A.; Lynch, J.P. The hidden half of crop yields. *Nat. Plants* **2015**, *1*, 15117. [[CrossRef](#)] [[PubMed](#)]
- Chen, J.; Zhang, Y.; Tan, Y.; Zhang, M.; Zhu, L.; Xu, G.; Fan, X. Agronomic nitrogen-use efficiency of rice can be increased by driving Os NRT 2.1 expression with the Os NAR 2.1 promoter. *Plant Biotechnol. J.* **2016**, *14*, 1705–1715. [[CrossRef](#)]
- Ruffel, S.; Gojon, A.; Lejay, L. Signal interactions in the regulation of root nitrate uptake. *J. Exp. Bot.* **2014**, *65*, 5509–5517. [[CrossRef](#)]
- Paez-Garcia, A.; Motes, C.M.; Scheible, W.; Chen, R.; Blancaflor, E.B.; Monteros, M.J. Root traits and phenotyping strategies for plant improvement. *Plants* **2015**, *4*, 334–355. [[CrossRef](#)]
- Osmont, K.S.; Sibout, R.; Hardtke, C.S. Hidden branches: Developments in root system architecture. *Annu. Rev. Plant Biol.* **2007**, *58*, 93–113. [[CrossRef](#)]
- Ju, C.; Buresh, R.J.; Wang, Z.; Zhang, H.; Liu, L.; Yang, J.; Zhang, J. Root and shoot traits for rice varieties with higher grain yield and higher nitrogen use efficiency at lower nitrogen rates application. *Field Crop Res.* **2015**, *175*, 47–55. [[CrossRef](#)]
- Duncan, E.G.; O’Sullivan, C.A.; Roper, M.M.; Palta, J.; Whisson, K.; Peoples, M.B. Yield and nitrogen use efficiency of wheat increased with root length and biomass due to nitrogen, phosphorus, and potassium interactions. *J. Plant Nutr. Soil Sci.* **2018**, *181*, 364–373. [[CrossRef](#)]
- Ping, W.; Wang, Z.; Cai, R.; Yong, L.L.; Chen, X.; Yin, Y. Physiological and molecular response of wheat roots to nitrate supply in seedling stage. *Agric. Sci. China* **2011**, *10*, 695–704. [[CrossRef](#)]
- Zhan, A.; Lynch, J.P. Reduced frequency of lateral root branching improves N capture from low-N soils in maize. *J. Exp. Bot.* **2015**, *66*, 2055–2065. [[CrossRef](#)]
- Saengwilai, P.; Strock, C.; Rangarajan, H.; Chimungu, J.; Salungyu, J.; Lynch, J.P. Root hair phenotypes influence nitrogen acquisition in maize. *Ann. Bot.* **2021**, *128*, 849–858. [[CrossRef](#)]
- Neumann, K.; Kobiljski, B.; Denčić, S.; Varshney, R.K.; Börner, A. Genome-wide association mapping: A case study in bread wheat (*Triticum aestivum* L.). *Mol. Breed.* **2011**, *27*, 37–58. [[CrossRef](#)]
- Korte, A.; Farlow, A. The advantages and limitations of trait analysis with GWAS: A review. *Plant Methods* **2013**, *9*, 29. [[CrossRef](#)]
- Li, F.; Xie, J.; Zhu, X.; Wang, X.; Zhao, Y.; Ma, X.; Zhang, Z.; Rashid, M.A.; Zhang, Z.; Zhi, L. Genetic basis underlying correlations among growth duration and yield traits revealed by GWAS in rice (*Oryza sativa* L.). *Front. Plant Sci.* **2018**, *9*, 650. [[CrossRef](#)]
- Li, X.; Guo, T.; Wang, J.; Bekele, W.A.; Sukumaran, S.; Vanous, A.E.; McNellie, J.P.; Tibbs-Cortes, L.E.; Lopes, M.S.; Lamkey, K.R. An integrated framework reinstating the environmental dimension for GWAS and genomic selection in crops. *Mol. Plant* **2021**, *14*, 874–887. [[CrossRef](#)]
- Li, X.; Zhou, Z.; Ding, J.; Wu, Y.; Zhou, B.; Wang, R.; Ma, J.; Wang, S.; Zhang, X.; Xia, Z. Combined linkage and association mapping reveals QTL and candidate genes for plant and ear height in maize. *Front. Plant Sci.* **2016**, *7*, 833. [[CrossRef](#)]
- Bo, K.; Wei, S.; Wang, W.; Miao, H.; Dong, S.; Zhang, S.; Gu, X. QTL mapping and genome-wide association study reveal two novel loci associated with green flesh color in cucumber. *BMC Plant Biol.* **2019**, *19*, 243. [[CrossRef](#)] [[PubMed](#)]
- He, Y.; Wu, D.; Wei, D.; Fu, Y.; Cui, Y.; Dong, H.; Tan, C.; Qian, W. GWAS, QTL mapping and gene expression analyses in Brassica napus reveal genetic control of branching morphogenesis. *Sci. Rep.* **2017**, *7*, 15971. [[CrossRef](#)]
- Guo, J.; Guo, J.; Li, L.; Bai, X.; Huo, X.; Shi, W.; Gao, L.; Dai, K.; Jing, R.; Hao, C. Combined linkage analysis and association mapping identifies genomic regions associated with yield-related and drought-tolerance traits in wheat (*Triticum aestivum* L.). *Theor. Appl. Genet.* **2023**, *136*, 250. [[CrossRef](#)] [[PubMed](#)]
- Sallam, A.; Eltahir, S.; Alqudah, A.M.; Belamkar, V.; Baenziger, P.S. Combined GWAS and QTL mapping revealed candidate genes and SNP network controlling recovery and tolerance traits associated with drought tolerance in seedling winter wheat. *Genomics* **2022**, *114*, 110358. [[CrossRef](#)]
- Yang, X.; Pan, Y.; Singh, P.K.; He, X.; Ren, Y.; Zhao, L.; Zhang, N.; Cheng, S.; Chen, F. Investigation and genome-wide association study for Fusarium crown rot resistance in Chinese common wheat. *BMC Plant Biol.* **2019**, *19*, 153. [[CrossRef](#)]

26. Basnet, B.R.; Singh, R.P.; Ibrahim, A.; Herrera-Foessel, S.A.; Huerta-Espino, J.; Lan, C.; Rudd, J.C. Characterization of Yr54 and other genes associated with adult plant resistance to yellow rust and leaf rust in common wheat Quaiu 3. *Mol. Breed.* **2014**, *33*, 385–399. [[CrossRef](#)]
27. Ponce-Molina, L.J.; Huerta-Espino, J.; Singh, R.P.; Basnet, B.R.; Alvarado, G.; Randhawa, M.S.; Lan, C.X.; Aguilar-Rincón, V.H.; Lobato-Ortiz, R.; García-Zavala, J.J. Characterization of leaf rust and stripe rust resistance in spring wheat ‘Chilero’. *Plant Dis.* **2018**, *102*, 421–427. [[CrossRef](#)]
28. Hoagland, D.R.; Arnon, D.I. The water-culture method for growing plants without soil. *Circular. Calif. Agric. Exp. Stn.* **1950**, *347*, 39.
29. Zhao, Y.; Yan, X.; Zeng, Z.; Zhao, D.; Chen, P.; Wang, Y.; Chen, F.; Wang, C. Integrated genome-wide association study and QTL mapping reveals qSa-3A associated with English grain aphid, *Sitobion avenae* (Fabricius) resistance in wheat. *Pest. Manag. Sci.* **2023**, *79*, 3970–3978. [[CrossRef](#)]
30. Lv, G.; Dong, Z.; Wang, Y.; Geng, J.; Li, J.; Lv, X.; Sun, C.; Ren, Y.; Zhang, J.; Chen, F. Identification of genetic loci of black point in Chinese common wheat by genome-wide association study and linkage mapping. *Plant Dis.* **2020**, *104*, 2005–2013. [[CrossRef](#)]
31. Niaz, M.; Zhang, L.; Lv, G.; Hu, H.; Yang, X.; Cheng, Y.; Zheng, Y.; Zhang, B.; Yan, X.; Htun, A. Identification of TaGL1-B1 gene controlling grain length through regulation of jasmonic acid in common wheat. *Plant Biotechnol. J.* **2023**, *21*, 979–989. [[CrossRef](#)] [[PubMed](#)]
32. Shi, H.; Chen, M.; Gao, L.; Wang, Y.; Bai, Y.; Yan, H.; Xu, C.; Zhou, Y.; Xu, Z.; Chen, J. Genome-wide association study of agronomic traits related to nitrogen use efficiency in wheat. *Theor. Appl. Genet.* **2022**, *135*, 4289–4302. [[CrossRef](#)]
33. Storey, J.; Bass, A.; Dabney, A.; Robinson, D. Package ‘qvalue’. *Medicine* **2011**, *344*, 539–548.
34. Liu, J.; He, Z.; Rasheed, A.; Wen, W.; Yan, J.; Zhang, P.; Wan, Y.; Zhang, Y.; Xie, C.; Xia, X. Genome-wide association mapping of black point reaction in common wheat (*Triticum aestivum* L.). *BMC Plant Biol.* **2017**, *17*, 220. [[CrossRef](#)] [[PubMed](#)]
35. Ren, Y.; Qian, Y.; Xu, Y.; Zou, C.; Liu, D.; Zhao, X.; Zhang, A.; Tong, Y. Characterization of QTLs for root traits of wheat grown under different nitrogen and phosphorus supply levels. *Front. Plant Sci.* **2017**, *8*, 2096. [[CrossRef](#)]
36. Yang, M.; Wang, C.; Hassan, M.A.; Wu, Y.; Xia, X.; Shi, S.; Xiao, Y.; He, Z. QTL mapping of seedling biomass and root traits under different nitrogen conditions in bread wheat (*Triticum aestivum* L.). *J. Integr. Agric.* **2021**, *20*, 1180–1192. [[CrossRef](#)]
37. Mapchart, V.E. software for the Graphical Presentation of Linkage Maps and QTLs. *J. Hered.* **2002**, *93*, 77r–78r.
38. McCouch, S.R.; CGSNL (Committee on Gene Symbolization, Nomenclature and Linkage, Rice Genetics Cooperative). Gene nomenclature system for rice. *Rice* **2008**, *1*, 72–84. [[CrossRef](#)]
39. Wang, Y.; Hou, J.; Liu, H.; Li, T.; Wang, K.; Hao, C.; Liu, H.; Zhang, X. TaBT1, affecting starch synthesis and thousand kernel weight, underwent strong selection during wheat improvement. *J. Exp. Bot.* **2019**, *70*, 1497–1511. [[CrossRef](#)]
40. Kong, D.L.; Wang, J.J.; Kardol, P.; Wu, H.F.; Zeng, H.; Deng, X.B.; Deng, Y. Economic strategies of plant absorptive roots vary with root diameter. *Biogeosciences* **2016**, *13*, 415–424. [[CrossRef](#)]
41. Xue, Y.; Zhang, W.; Liu, D.; Yue, S.; Cui, Z.; Chen, X.; Zou, C. Effects of nitrogen management on root morphology and zinc translocation from root to shoot of winter wheat in the field. *Field Crop Res.* **2014**, *161*, 38–45. [[CrossRef](#)]
42. Zhang, H.; Jennings, A.; Barlow, P.W.; Forde, B.G. Dual pathways for regulation of root branching by nitrate. *Proc. Natl. Acad. Sci. USA* **1999**, *96*, 6529–6534. [[CrossRef](#)] [[PubMed](#)]
43. Xiong, H.; Guo, H.; Zhou, C.; Guo, X.; Xie, Y.; Zhao, L.; Gu, J.; Zhao, S.; Ding, Y.; Liu, L. A combined association mapping and *t*-test analysis of SNP loci and candidate genes involving in resistance to low nitrogen traits by a wheat mutant population. *PLoS ONE* **2019**, *14*, e211492. [[CrossRef](#)] [[PubMed](#)]
44. An, D.; Su, J.; Liu, Q.; Zhu, Y.; Tong, Y.; Li, J.; Jing, R.; Li, B.; Li, Z. Mapping QTLs for nitrogen uptake in relation to the early growth of wheat (*Triticum aestivum* L.). *Plant Soil* **2006**, *284*, 73–84. [[CrossRef](#)]
45. Erenoglu, E.B.; Kutman, U.B.; Ceylan, Y.; Yildiz, B.; Cakmak, I. Improved nitrogen nutrition enhances root uptake, root-to-shoot translocation and remobilization of zinc (65Zn) in wheat. *New Phytol.* **2011**, *189*, 438–448. [[CrossRef](#)]
46. Wei, H.; Zhang, H.; Zhang, S.; Jie, H. Root Morphological and Physiological Characteristics in Rice Genotypes with Different N Use Efficiencies. *Acta Agron. Sin.* **2008**, 429–436. [[CrossRef](#)]
47. Fan, X.; Zhang, W.; Zhang, N.; Chen, M.; Zheng, S.; Zhao, C.; Han, J.; Liu, J.; Zhang, X.; Song, L. Identification of QTL regions for seedling root traits and their effect on nitrogen use efficiency in wheat (*Triticum aestivum* L.). *Theor. Appl. Genet.* **2018**, *131*, 2677–2698. [[CrossRef](#)]
48. Zuo, W.; Chao, Q.; Zhang, N.; Ye, J.; Tan, G.; Li, B.; Xing, Y.; Zhang, B.; Liu, H.; Fengler, K.A. A maize wall-associated kinase confers quantitative resistance to head smut. *Nat. Genet.* **2015**, *47*, 151–157. [[CrossRef](#)]
49. Zandipour, M.; Majidi Hervan, E.; Azadi, A.; Khosroshahli, M.; Etmian, A. A QTL hot spot region on chromosome 1B for nine important traits under terminal drought stress conditions in wheat. *Cereal Res. Commun.* **2020**, *48*, 17–24. [[CrossRef](#)]
50. Tura, H.; Edwards, J.; Gahlaut, V.; Garcia, M.; Sznajder, B.; Baumann, U.; Shahinnia, F.; Reynolds, M.; Langridge, P.; Balyan, H.S. QTL analysis and fine mapping of a QTL for yield-related traits in wheat grown in dry and hot environments. *Theor. Appl. Genet.* **2020**, *133*, 239–257. [[CrossRef](#)]
51. Zhang, Q.; Wei, W.; Zuansun, X.; Zhang, S.; Wang, C.; Liu, N.; Qiu, L.; Wang, W.; Guo, W.; Ma, J. Fine mapping of the leaf rust resistance gene Lr65 in spelt wheat ‘Altgold’. *Front. Plant Sci.* **2021**, *12*, 666921. [[CrossRef](#)] [[PubMed](#)]
52. Hitz, K.; Clark, A.J.; Van Sanford, D.A. Identifying nitrogen-use efficient soft red winter wheat lines in high and low nitrogen environments. *Field Crop Res.* **2017**, *200*, 1–9. [[CrossRef](#)]

53. Cui, F.; Zhao, C.; Ding, A.; Li, J.; Wang, L.; Li, X.; Bao, Y.; Li, J.; Wang, H. Construction of an integrative linkage map and QTL mapping of grain yield-related traits using three related wheat RIL populations. *Theor. Appl. Genet.* **2014**, *127*, 659–675. [[CrossRef](#)] [[PubMed](#)]
54. Fontaine, J.; Ravel, C.; Pageau, K.; Heumez, E.; Dubois, F.; Hirel, B.; Le Gouis, J. A quantitative genetic study for elucidating the contribution of glutamine synthetase, glutamate dehydrogenase and other nitrogen-related physiological traits to the agronomic performance of common wheat. *Theor. Appl. Genet.* **2009**, *119*, 645–662. [[CrossRef](#)] [[PubMed](#)]
55. Guo, Y.; Kong, F.; Xu, Y.; Zhao, Y.; Liang, X.; Wang, Y.; An, D.; Li, S. QTL mapping for seedling traits in wheat grown under varying concentrations of N, P and K nutrients. *Theor. Appl. Genet.* **2012**, *124*, 851–865. [[CrossRef](#)]
56. Ren, D.; Fang, X.; Jiang, P.; Zhang, G.; Hu, J.; Wang, X.; Meng, Q.; Cui, W.; Lan, S.; Ma, X. Genetic architecture of nitrogen-deficiency tolerance in wheat seedlings based on a nested association mapping (NAM) population. *Front. Plant Sci.* **2018**, *9*, 845. [[CrossRef](#)]
57. Saini, D.K.; Chopra, Y.; Pal, N.; Chahal, A.; Srivastava, P.; Gupta, P.K. Meta-QTLs, ortho-MQTLs and candidate genes for nitrogen use efficiency and root system architecture in bread wheat (*Triticum aestivum* L.). *Physiol. Mol. Biol. Plants* **2021**, *27*, 2245–2267. [[CrossRef](#)]
58. Yang, Y.; Amo, A.; Wei, D.; Chai, Y.; Zheng, J.; Qiao, P.; Cui, C.; Lu, S.; Chen, L.; Hu, Y. Large-scale integration of meta-QTL and genome-wide association study discovers the genomic regions and candidate genes for yield and yield-related traits in bread wheat. *Theor. Appl. Genet.* **2021**, *134*, 3083–3109. [[CrossRef](#)]
59. Liu, H.; Mullan, D.; Zhang, C.; Zhao, S.; Li, X.; Zhang, A.; Lu, Z.; Wang, Y.; Yan, G. Major genomic regions responsible for wheat yield and its components as revealed by meta-QTL and genotype–phenotype association analyses. *Planta* **2020**, *252*, 65. [[CrossRef](#)]
60. Zhang, H.; Forde, B.G. An Arabidopsis MADS box gene that controls nutrient-induced changes in root architecture. *Science* **1998**, *279*, 407–409. [[CrossRef](#)]
61. Remans, T.; Nacry, P.; Pervent, M.; Filleur, S.; Diatloff, E.; Mounier, E.; Tillard, P.; Forde, B.G.; Gojon, A. The Arabidopsis NRT1.1 transporter participates in the signaling pathway triggering root colonization of nitrate-rich patches. *Proc. Natl. Acad. Sci. USA* **2006**, *103*, 19206–19211. [[CrossRef](#)] [[PubMed](#)]
62. Yu, L.; Miao, Z.; Qi, G.; Wu, J.; Cai, X.; Mao, J.; Xiang, C. MADS-box transcription factor AGL21 regulates lateral root development and responds to multiple external and physiological signals. *Mol. Plant* **2014**, *7*, 1653–1669. [[CrossRef](#)] [[PubMed](#)]
63. Lei, L.; Li, G.; Zhang, H.; Powers, C.; Fang, T.; Chen, Y.; Wang, S.; Zhu, X.; Carver, B.F.; Yan, L. Nitrogen use efficiency is regulated by interacting proteins relevant to development in wheat. *Plant Biotechnol. J.* **2018**, *16*, 1214–1226. [[CrossRef](#)] [[PubMed](#)]
64. Wang, M.; Zhang, P.; Liu, Q.; Li, G.; Di, D.; Xia, G.; Kronzucker, H.J.; Fang, S.; Chu, J.; Shi, W. TaANR1-TaBG1 and TaWabi5-TaNRT2s/NARs link ABA metabolism and nitrate acquisition in wheat roots. *Plant Physiol.* **2020**, *182*, 1440–1453. [[CrossRef](#)] [[PubMed](#)]
65. He, X.; Qu, B.; Li, W.; Zhao, X.; Teng, W.; Ma, W.; Ren, Y.; Li, B.; Li, Z.; Tong, Y. The nitrate-inducible NAC transcription factor TaNAC2-5A controls nitrate response and increases wheat yield. *Plant Physiol.* **2015**, *169*, 1991–2005. [[CrossRef](#)]
66. Craig, A.; Ewan, R.; Mesmar, J.; Gudipati, V.; Sadanandom, A. E3 ubiquitin ligases and plant innate immunity. *J. Exp. Bot.* **2009**, *60*, 1123–1132. [[CrossRef](#)]
67. Park, G.; Park, J.; Yoon, J.; Yu, S.; An, G. A RING finger E3 ligase gene, *Oryza sativa* Delayed Seed Germination 1 (OsDSG1), controls seed germination and stress responses in rice. *Plant Mol. Biol.* **2010**, *74*, 467–478. [[CrossRef](#)]

Disclaimer/Publisher’s Note: The statements, opinions and data contained in all publications are solely those of the individual author(s) and contributor(s) and not of MDPI and/or the editor(s). MDPI and/or the editor(s) disclaim responsibility for any injury to people or property resulting from any ideas, methods, instructions or products referred to in the content.